Geocarto International

ISSN: 1010-6049 (Print) 1752-0762 (Online) Journal homepage: https://www.tandfonline.com/loi/tgei20

Object-based classification of mixed forest types in Mongolia

E. Nyamjargal, D. Amarsaikhan, A. Munkh-Erdene, V. Battsengel & Ch. Bolorchuluun

GEOCARTO INTERNATIONAL
https://doi.org/10.1080/10106049.2019.1583775

Object-based classification of mixed forest types in Mongolia

E. Nyamjargal[a], D. Amarsaikhan[a], A. Munkh-Erdene[a], V. Battsengel[b] and Ch. Bolorchuluun[b]

[a]Division of RS and Spatial Modelling, Institute of Geography and Geoecology, Mongolian Academy of Sciences, Ulaanbaatar, Mongolia; [b]Laboratory of RS and GIS, Department of Geography, National University of Mongolia, Ulaanbaatar, Mongolia

ABSTRACT

The aim of this study is to produce updated forest map of the Bogdkhan Mountain, Mongolia using multitemporal Sentinel-2A images. The target area has highly mixed forest types and it is very difficult to differentiate the fuzzy boundaries among different forest types. To extract the forest class information, an object-based classification technique is applied and a rule-base to separate the mixed classes is developed. The rule-base uses a hierarchy of rules describing different conditions under which the actual classification has to be performed. To compare the result of the developed method with a result of a pixel-based approach, a Bayesian maximum likelihood classification is applied. The final result indicates overall accuracy of 90.87% for the object-based classification, while for the pixel-based approach it is 79.89%. Overall, the research indicates that the object-based method that uses a thoroughly defined segmentation and a well-constructed rule-base can significantly improve the classification of mixed forest types and produce of a reliable forest map.

ARTICLE HISTORY
Received 1 October 2018
Accepted 2 February 2019

KEYWORDS
Object-based; rule-base; forest type; Sentinel-2A image

1. Introduction

Traditionally, satellite remote sensing (RS) data sets with different spectral, spatial and temporal resolutions have been efficiently used for a land cover analysis (Yan et al. 2015). Image classification is one of the widely used RS data processing methods. For several decades, pixel-based classification techniques have been extensively used for a thematic mapping of RS images (Amarsaikhan et al. 2012). They mainly used either a supervised classification, unsupervised classification or some of their combinations (Enderle and Weih 2005; Amarsaikhan et al. 2010). The pixel-based methods analyze the spectral properties of every pixel within the selected image frame, without taking into account some important characteristics related to the pixel of interest. With the growing availability of more data sets, other properties, including the spatial or contextual information could be effectively used to produce more accurate classification results (Dwivedi et al. 2004; Weih and Riggan 2012; Makinde et al. 2016).

Over the past few years, object-based classifications have been increasingly used for different mapping applications. These methods have been developed in order to improve

CONTACT D. Amarsaikhan amarsaikhan@mas.ac.mn

the traditional pixel-based classification techniques. Unlike the pixel-based classifications that are based on the information of each pixel in the data, the object-based classifications are based on the information from a set of similar pixels called image objects. The image objects are groups of pixels that are similar to one another based on the spectral properties, size, shape, and texture, as well as context from a neighborhood surrounding the pixels. The object-based method uses a segmentation process and iterative learning algorithm to achieve a semi-automatic classification procedure that demonstrates more accurate results than traditional pixel-based methods (Grenzdörffer 2005; Hay and Castilla 2006, Liu and Xia 2010; Weih and Riggan 2012).

In recent years, object-based methods have been successfully used for a forest mapping. Many authors applied these techniques for the identification of forest classes. Kim et al. (2009) investigated that segmentation quality, associated with the segmentation scale directly influence the classification result of forest types using optical imagery. In their method, an improved classification result of forest types, including deciduous broadleaf, evergreen coniferous and mixed forests, was achieved. Hajek (2014) classified the tree species from RS imagery based on the relative border to neighboring objects, relative area of sub-objects and shape with an accuracy of 94.5%. Martin and Lucie (2014) performed a forest type mapping by combining multispectral and LiDAR data using object-based classification approach. They established a set of rules using 26 indices, DSM, DTM and LiDAR data and classified the forested areas with an accuracy of 89.5%. Mitchell et al. (2016) developed a forest classification process and correctly separated the forested area using spectral band ratios, NDVI, SLAVI and NDWI.

The Mongolian forests are mainly located in the northern parts of the country along the Russian border forming a transition zone between the Siberian taiga forest and the Central Asian steppe zones (Tsogtbaatar 2002). In the past, total forest related area of Mongolia constituted about 17.5 million ha or 11.2% of the total land area. The area of potentially exploitable forest was estimated to be between 5 and 6 million ha. The average growing stock in the northern forests varied between 54 and 79 cubic meters/ha in the whole forest area, and between 100 and 154 cubic meters/ha in the exploitable forests. The total growing stock was 1.3 billion cubic meters and the exploitable volume was 6 million cubic meters (Mongolian Forestry Sector, 1998). However, recently, forest land degradation has become the main concern in the country. It has been found that much of the existing forests have been destroyed, mainly by timber preparation, legal and illegal logging, forest fires and careless human activities. To account all of these changes, forest specialists need to have an updated forest map. As the present RS techniques and methods are so advanced, it is possible to produce a reliable forest map and use it for planning and management (Amarsaikhan et al. 2011; Enkhjargal et al. 2015).

The aim of this study is to classify highly mixed forest types and produce a reliable forest map of the Bogdkhan Mountain, Mongolia using multitemporal optical Sentinel-2A images. To extract the forest class information, an object-based classification technique based on a multi-resolution segmentation and constructed rule-base have been applied. The classification result of the object-based method was compared with a result of a standard Bayesian maximum likelihood classification and it demonstrated a higher accuracy.

2. Test area and data sources

As a test site, Bogdkhan Mountain, a nature protected area, situated in Central Mongolia, near the capital city of Ulaanbaatar has been selected. It is a protected area and has a

Table 1. Characteristics of spectral bands of Sentinel-2A.

Band	Wavelength (μm)	Spatial resolution (m)	Bandwidth (nm)
Band 1	0.443	60	27/45 (2A/2B)
Band 2	0.490	10	98
Band 3	0.560	10	45/46 (2A/2B)
Band 4	0.665	10	38/39 (2A/2B)
Band 5	0.705	20	19/20 (2A/2B)
Band 6	0.740	20	18
Band 7	0.783	20	28
Band 8	0.842	10	115
Band 8a	0.865	20	20
Band 9	0.945	60	20
Band 10	1.375	60	20
Band 11	1.610	20	90
Band 12	2.190	20	180

territory of 41,651 ha, of which 55% is covered by highly mixed forest types. The mountain has 588 species of high plants, which are related to 256 geneses of 70 families. 135 species such as carex, artemisa, oxytropis that relate to 11 main geneses comprise 22.9% of all species distributed on the mountain. Forest is distributed on the altitude range of 1400 m (1450m)-2100m (2150m) above sea level and consists of three sub zones such as mountain plateau, taiga and taiga type. Cedar and larch dominate in the forest cover but pine, birch, spruce and willow also occur (Enkhjargal et al. 2015). The forest area of the mountain is extended from the west to the east about 29 km and from the north to the south about 18 km.

In the current study, the satellite data used consisted of geocoded Sentinel-2A multispectral images acquired on 13 August and 15 October of 2016. As the test area has highly mixed forest classes, such multitemporal data sets are important for differentiation among different deciduous and coniferous forest types. Sentinel-2A images have 12 spectral bands (Sentinel-2 User Handbook 2015) and their characteristics are presented in Table 1. In addition, a forest taxonomy map of scale 1:100.000 and some ground truth data were available. Figure 1 shows multitemporal Sentinel-2A images of the Bogdkhan Mountain.

3. Results and discussion

In the object-based method, after an image is segmented into appropriate image objects, the image is classified by assigning each object to a class, based on features and criteria set by the user. To obtain useful information, the segmentation process splits an image into unclassified 'object primitives' that form the basis for the image objects. Segmentations, and the resulting characteristics of object primitives and eventual image objects are based on shape, size, color, and pixel topology controlled through parameters set by the user. The values of the parameters define how much influence spectral and spatial characteristics of the image layers will have in defining the shape and size of the image objects. The user modifies the settings depending on the objective of the study, as well as the image quality, available bands and image resolution. As a general rule, reliable image objects should be as large as possible, but small enough to show details of interest (Gronemeyer 2012).

In the current study, the object-based classification of forest types consists of three processes, namely, segmentation, rule-based classification and accuracy assessment.

Figure 1. Sentinel-2A images of the test area acquired on 13 August (a) and 15 October (b) of 2016.

3.1. Segmentation process

It starts by segmenting the selected RS data using a multi-resolution segmentation. The multi-resolution segmentation is one of the well-known methods (Hofmann 2001). It uses the following parameters:

- Scale parameter: influence the average object size and it determines the maximal allowed heterogeneity of the objects. The larger scale parameter, the larger objects become.
- Shape/Color: adjust the influence of shape vs. color homogeneity on the object generation. The higher the shape value, the less spectral homogeneity influences the object generation.
- Smoothness/Compactness: determine the compactness or smoothness of the resulting object.

The segmentation parameters to be selected by the user are interrelated to each other. It is impossible to directly find a set of proper segmentation parameters at one time. Users have to repeatedly select a set of segmentation parameters and test them through a trial-and-error process, until a reasonable segmentation result is achieved or the user does not want to continue the trial and error anymore (Zhang et al. 2010). In our study, shape, color, smoothness and compactness were selected by increasing and decreasing each of the parameters to find the best values that would control the appropriate segmentation. After many tests, the parameters: scale, shape and compactness were set as 70, 0.2 and 0.5, respectively. Figure 2 shows a result of the applied multi-resolution segmentation.

As seen from Figure 2, the image objects have been created by combining similar pixels based on their properties, and 99,428 image objects were created. In the figure, the darker image objects belong to the evergreen and coniferous forest types, whereas the light green ones imply to the deciduous forest classes. Moreover, it is seen that it could be difficult to determine the fuzzy boundary between the evergreen and deciduous forests if a scale of the segmentation process was not proper. Defining too small scale factor might cause a salt-and-pepper error. Meanwhile, if a larger scale factor is defined, the border of forest types could not be clear and accurate. Thus, the segmentation parameters selected for the present analysis were appropriate and the image objects were distinctive.

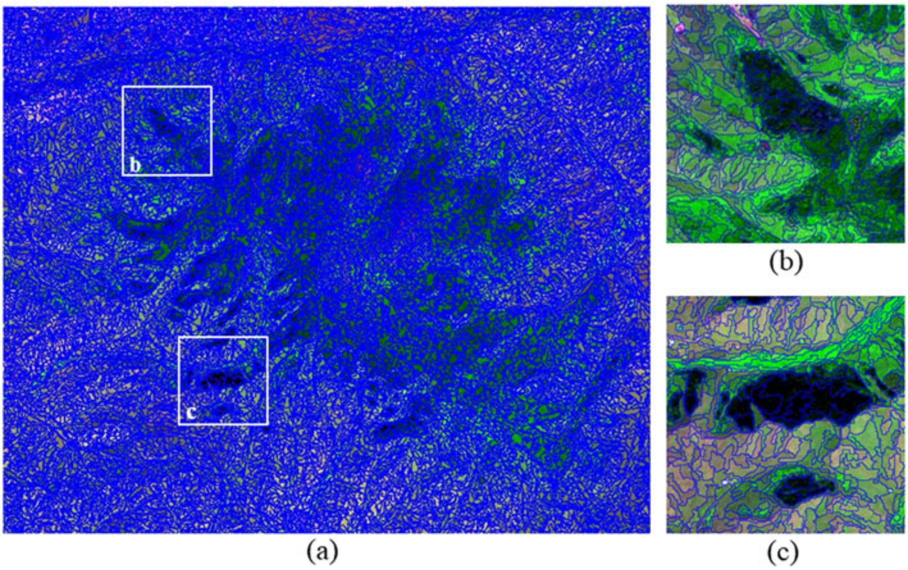

Figure 2. Result of the multi-resolution segmentation: (a) segmentation of the Bogdkhan Mountain, (b,c) details showing the image objects.

3.2. Rule-based classification of the forest types

After the segmentation, the image objects have been classified into the selected forest classes, using the constructed rules. To achieve a reliable classification result, initially, the entire image had to be divided into 'vegetation' and 'non-vegetation' classes. Then, the 'vegetation' class had been sub-divided into 'grass' and 'forest' classes. After that 'forest' class was classified into 'evergreen forest' and 'deciduous forest'. As a final procedure, the 'evergreen forest' was classified into 'spruce', 'pine' and 'cedar' classes. Meanwhile, the deciduous forest was classified into 'birch', 'larch' and 'willow' classes. A general diagram of the applied object-based classification technique is shown in Figure 3.

In order to collect statistical information about the available forest classes to be used for a rule-base, the training samples have been selected from the mean spectral values of 11 bands (B2, B3, B4, B5, B6, B7, B8, B8A, B10, B11 and B12) of the selected Sentinel images based on the field measurements and ground truth information. Table 2 shows the area size of forest types and selected number of training samples.

As seen from Table 2, more than half of the forested areas (i.e. about 62.1%) of the Bogdkhan Mountain constitutes a larch forest. The training samples of the classes were selected on a principle that more pixels to be selected for the larger classes, such as larch and cedar, than the smaller classes, such as pine and willow.

To perform a rule-based classification, six different types of indices such as green leaf algorithm (GLA), normalized difference of vegetation indices (NDVI), simple ratio, ratio of red and green bands, ratio of red and NIR bands and ratio of NIR and SWIR bands have been estimated for the multitemopral images and they were identified as 'Aug.' and 'Oct.' indices. The equations used to calculate the indices are shown in Table 3. Eventually, a set of rules forming rule-base was developed based on the threshold values using six indices and the training samples for forest classes and the area of image objects. A diagram showing rules of the developed rule-base is presented in Figure 4.

It is seen from Figure 4 that for the separation of 'vegetation' and 'non-vegetation' classes the rules that use the growing season NDVI and ratio of red and NIR bands have

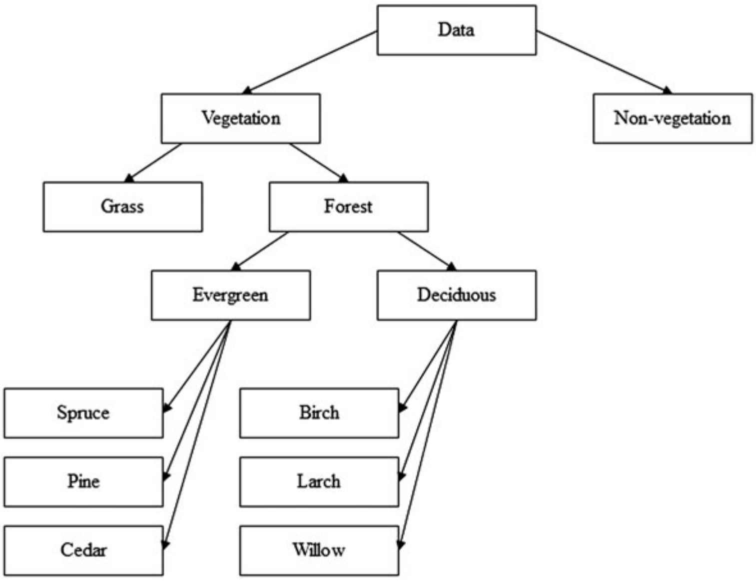

Figure 3. A general diagram of the constructed object-based classification method.

Table 2. Area size of forest types and the selected number of training samples.

Forest type	Area size (sq.m)	Percentage (%)	Number of training samples (pixels)
Spruce	17 040 942.827	8.9	192
Cedar	45 934 635.429	23.9	288
Pine	3 782 412.011	2.0	172
Birch	5 290 909.372	2.8	144
Larch	119 337 123.875	62.1	508
Willow	634 352.277	0.3	56
	192 020 375.791	100	1360

Table 3. The used indices and related equations.

Indices	Equation
GLA (Green Leaf Algorithm)	(2 * Green - Red - Blue) / (2 * Green + Red + Blue)
NDVI (Normalized Vegetation Index)	(NIR - Red) / (NIR + Red)
B8 / B4 (Simple ratio)	NIR / Red
B4 / B3 (ratio of red and green bands)	Red / Green
B4 / B8 (ratio of red and NIR bands)	Red / NIR
B8 / B11 (ratio of NIR and SWIR bands)	NIR / SWIR 1

been applied. The defined ‘vegetation’ class has been divided into ‘forest’ and ‘grass’ classes using the rules, set in the ratio of red and green bands and mean narrow NIR value of the August imagery. Then, differentiation between the ‘evergreen’ and ‘deciduous’ forests was performed using criteria, set in a GLA estimated for the October image and ratio of red and green bands. After that ‘evergreen’ forest was classified into ‘spruce’, ‘pine’ and ‘cedar’ classes, while ‘deciduous’ forest was classified into ‘birch’, ‘larch’ and ‘willow’ classes applying the rules that use different indices and threshold values. The final classification result is shown in Figure 5.

3.3. Pixel-based classification of the forest types

Until the development of advanced classification methods such as object-based or knowledge-based techniques, pixel-based approaches have been widely used for a variety of

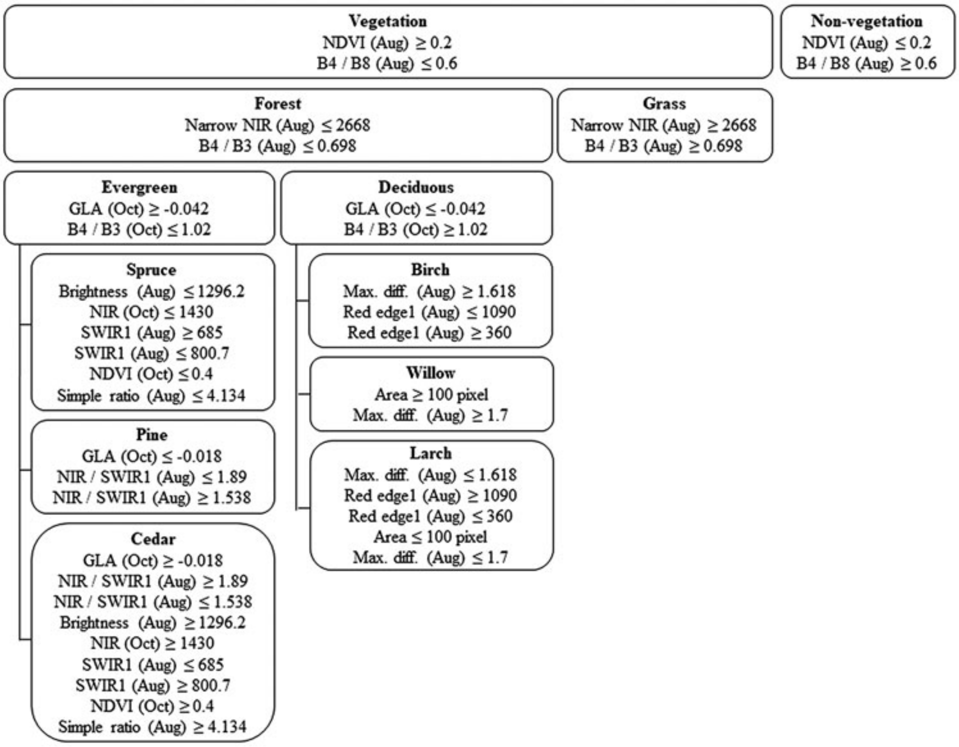

Figure 4. A diagram of the constructed rules in the rule-base.

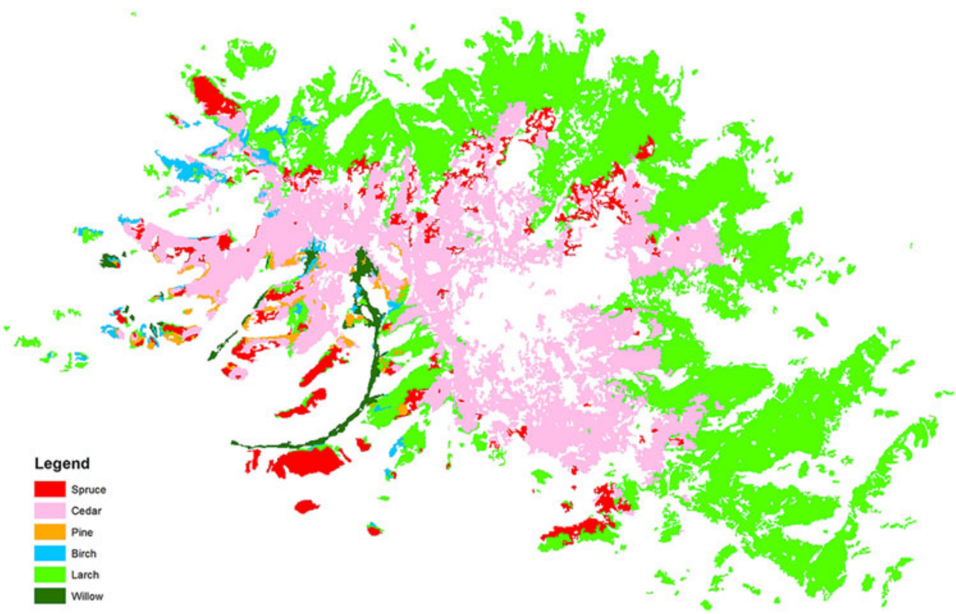

Figure 5. Final result of the object-based classification.

thematic mapping applications. In the pixel-based classification, individual image pixels are analyzed by their spectral information that they contain. Unlike the object-based methods, pixel-based classifications do not use the information from surrounding pixels, which may help in correctly identifying the target pixel's class. In such a case, a class that displays high spectral heterogeneity may have its pixels labelled as different classes (Piazza et al. 2016).

In our study, as a standard pixel-based method, a Bayesian statistical maximum likelihood classification has been used assuming that the training samples have the Gaussian distribution. The basis of a maximum likelihood classification is the actual frequencies of co-occurrence between class (C_i) and an observation vector (x). In the case of multidimensional RS data, we assume that each observation x (pixel) consists of a set of measurements on N variables (features) (Amarsaikhan and Ganchuluun 2015). The decision rule, assuming Bayes' rule, can be written as follows:

$$P(Ci|x) = P(x|Ci) * P(Ci)/P(x)$$

where P(Ci|x)-posterior probability, P(x|Ci)-conditional probability, P(Ci)-prior probability, P(x)-probability of finding a pixel from any class. The actual classification is performed according to $P(Ci|x) > P(Cj|x)$ for all j#i.

In the current study, for the available classes, as each of them has different area size, the following prior probabilities have been used:

$$\begin{gathered} P(\text{spruce}) = 0.09 \\ P(\text{cedar}) = 0.24 \\ P(\text{pine}) = 0.02 \\ P(\text{birch}) = 0.03 \\ P(\text{larch}) = 0.61 \\ P(\text{willow}) = 0.01 \end{gathered}.$$

As the cedar and larch forests have larger area sizes in the target area than the other classes, to these classes higher prior probabilities were assigned. The rule has the maximum benefit of correct classification, because a pixel classified by this method has the maximum probability of correct assignment. Therefore, the method is considered as one of the most efficient methods for statistical pattern recognition (Erbek et al. 2004).

To conduct a Bayesian classification, initially, from the Sentinel image, several areas of interest (AOI)s representing the selected forest classes have been selected. The separability of the training signatures was firstly checked in feature space. After checking the signatures in feature space, they were evaluated using Jeffries–Matusita distance. The values of Jeffries–Matusita distance range from 0 to 2.0 and indicate how well the selected pairs are statistically separate. The values greater than 1.9 indicate that the pairs have good separability (ERDAS 2010). After the investigation, the samples that demonstrated the greatest separability were chosen to form the final signatures. The final classified image using the pixel-based approach is shown in Figure 6.

3.4. Accuracy assessment of the classification results

Generally, accuracy assessment is required for evaluating the quality of the performed classification results or for identifying a suitable classification method by comparing different classification outputs in a selected study area (Moran 2010). An error matrix is the most frequently used approach in accuracy assessment from which other important accuracy assessment elements, such as overall classification accuracy (OCA), producer's accuracy (PA), user's accuracy (UA) and Kappa coefficient (KC) can be derived (Wulder et al. 2006; Foody 2009; Li et al. 2011).

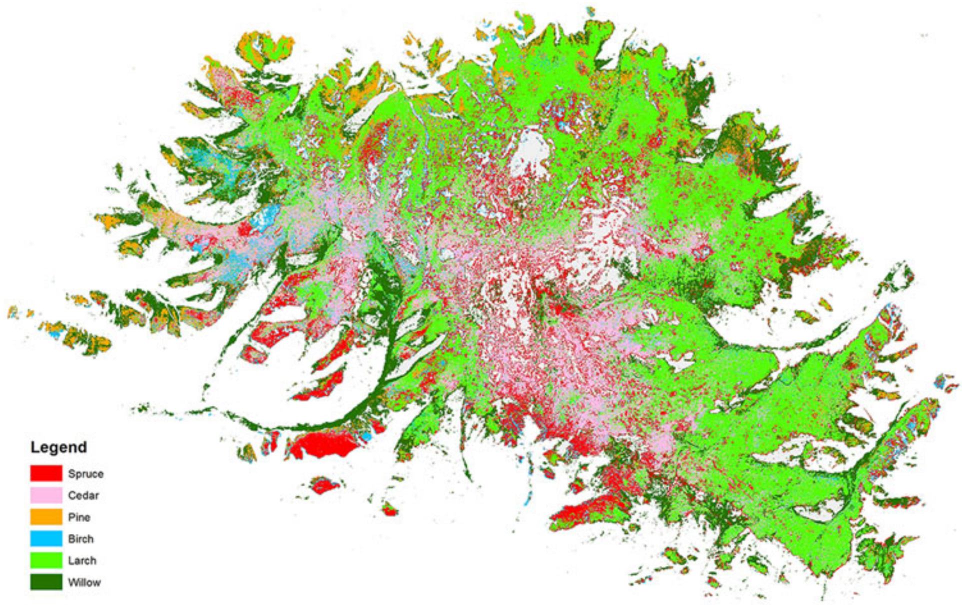

Figure 6. Result of the pixel-based classification.

OCA calculates the total number of correctly classified class without taking into account the omission and commission errors, thus it does not reveal whether errors were evenly distributed between classes or whether some classes were really bad and some really good. The KC is a measure of overall statistical agreement of an error matrix, which takes non-diagonal elements into account. The analysis based on KC is considered as a powerful technique for analyzing a single error matrix and for comparing differences between various error matrices (Foody 2004). Both OCA and OKC reflect the overall classification situation that cannot provide the reliability of some classes of interest, hence, PA and UA for each available class are often used to provide the complementary analysis of the accuracy assessment (Li et al. 2011).

In the present study, the accuracy assessments have been performed based on the sample pixels defined from field survey measurements as well as available ground truth information. In case of the object-based method 3341 pure pixels, while in case of the pixel-based technique 3317 pure pixels had been selected, accordingly. Error matrices have been created for the two classification results and then for each of them the OCA, PA, UA and KC were calculated from the corresponding matrix. The classification accuracies of the selected classes for both methods are shown in Tables 4 and 5.

As seen from the tables, the OCA and KC are 90.87% and 0.8688 for the object-based technique, whereas they are 79.89% and 0. 7579 for the maximum likelihood classification, respectively. The PA assessment results of all forest classes exceed 82.33% for the object-based classification, while the 'cedar' and 'pine' forests demonstrate lowest results in the pixel-based approach compared to other classes. In case of the UA assessment, the 'spruce' forest showed a lower percentage of accuracy for the object-based classification. For the standard method, 'pine' forest demonstrates the worst result and its UA is just 24.07%. As seen from the classified images and evaluated accuracies, the result of the object-based technique is much better than the result of the traditional method.

Table 4. Accuracy assessment for the object-based classification.

	Larch	Cedar	Spruce	Willow	Birch	Pine	Total
Ground truth pixels							
Larch	1330	17	48	0	0	0	1395
Cedar	1	1035	0	0	0	0	1036
Spruce	96	85	247	0	24	14	466
Willow	0	15	5	199	0	0	219
Birch	0	0	0	0	112	0	112
Pine	0	0	0	0	0	113	113
Total	1427	1152	300	199	136	127	3341
Accuracy							
Producer (%)	93.20	89.84	82.33	100	82.35	88.98	
User (%)	95.34	99.90	53.00	90.87	100	100	
Overall accuracy (%): 90.87							
Kappa coefficient: 0.8688							

Table 5. Accuracy assessment for the pixel-based classification.

	Larch	Cedar	Spruce	Willow	Birch	Pine	Total
Ground truth pixels							
Larch	930	75	10	0	2	12	1029
Cedar	99	679	1	0	2	17	798
Spruce	52	9	493	0	0	3	557
Willow	54	2	0	239	5	0	300
Birch	21	6	0	10	218	0	255
Pine	76	197	14	0	0	91	378
Total	1232	968	518	249	227	123	3317
Accuracy							
Producer (%)	75.48	70.14	95.17	95.98	96.04	73.98	
User (%)	90.37	85.09	88.50	79.66	85.49	24.07	
Overall accuracy (%): 79.89							
Kappa coefficient: 0.7579							

4. Conclusions

The aim of the research was to produce a reliable forest map using multitemporal optical Sentinel-2A images. As a test site, Bogdkhan Mountain with highly mixed forest types, situated in Central Mongolia was selected. For the extraction of the forest class information, the object-based classification technique was applied. To derive the thematic information, initially, to the selected RS images multi-resolution segmentation was applied. Then, the obtained image objects were classified into different forest classes using the developed rule-base. The rule-base contained a hierarchy of rules, describing different conditions under which the actual classification should to be accomplished. The result of the object-based technique was evaluated using four different accuracy assessment methods and it indicated overall accuracy of 90.87%. To compare the result of the developed method with the result of a standard approach, the Bayesian maximum likelihood classification was used. The result of the pixel-based approach was also evaluated using the four accuracy assessment methods it demonstrated overall accuracy of 79.89%. As seen from the analysis, the research indicated that the object-based technique, based on the thoroughly defined image segmentation and well-constructed rule-base could significantly improve the classification of mixed forest classes and production of the forest map.

References

Amarsaikhan D, Battsengel V, Amarjargal SH, Egshiglen E, Ganzorig M, Enkhjargal D. 2011. Applications of optical and microwave RS for forest mapping in Mongolia, Full paper published in CD-ROM Proceedings of the ACRS, Taipei, Taiwan.

Amarsaikhan D, Blotevogel HH, van Genderen JL, Ganzorig M, Gantuya R, Nergui B. 2010. Fusing high resolution TerraSAR and Quickbird images for urban land cover study in Mongolia. Int J Image Data Fusion. 1(1):83–97.

Amarsaikhan D, Ganzorig M, Saandar M, Blotevogel HH, Egshiglen E, Gantuya R, Nergui B, Enkhjargal D. 2012. Comparison of multisource image fusion methods and land cover classification. Int J Remote Sens. 33(8):2532–2550.

Amarsaikhan D, Ganchuluun N. 2015. Chapter 4 – "Fusion and Classification of Multisource Images for Update of Forest GIS". In *Image fusion: Principles, technology and applications*. New York: Nova Science Publishers, pp. 83–121.

Dwivedi RS, Kandrika S, Ramana KV. 2004. Comparison of classifiers of remote-sensing data for land-use/land-cover mapping. Curr Sci. 86(2):328–335.

Enderle D, Weih RC. Jr. 2005. Integrating supervised and unsupervised classification methods to develop a more accurate land cover classification. J Ark Acad Sci. 59:65–73.

Enkhjargal D, Amarsaikhan D, Bolor G, Tsetsegjargal N, Tsogzol G. 2015. Forest mapping in Mongolia using optical and SAR images. Full paper published in CD-ROM Proceedings of the ACRS, Manila, Philippines.

Erbek FS, Zkan CO, Taberner M. 2004. Comparison of maximum likelihood classification method with supervised artificial neural network algorithms for land use activities. Int J Remote Sens. 25(9): 1733–1748.

ERDAS 2010. New ERDAS Field Guide, Atlanta, Georgia: ERDAS, Inc., pp. 776.

Foody GM. 2004. Thematic map comparison: evaluating the statistical significance of differences in classification accuracy. Photogramm Eng Remote Sensing. 70(5):627–633.

Foody GM. 2009. Classification accuracy comparison: Hypothesis tests and the use of confidence intervals in evaluations of difference, equivalence and non2inferiority. Remote Sens Environ. 113(8):1658–1663.

Grenzdörffer GJ. 2005. Land use change in Rostock, Germany since the reunification-a combined approach with satellite data and high resolution aerial images, *Proceedings of the ISPRS WG VII/ 1'Human Settlements and Impact Analysis'-3rd International Symposium Remote Sensing and Data Fusion over Urban Areas (Urban 2005) and 5th International Symposium Remote Sensing of Urban Areas* (URS 2005), 14–16 March 2005, Tempe, Arizona.

Gronemeyer P. 2012. Object-based classification, The Landscape Tool Box, available at: http://wiki.landscapetoolbox.org/doku.php/remote_sensing_methods:object-based_classification.

Hajek F. 2014. Object-Oriented classification of remote sensing data for the identification of tree species composition, https://www.researchgate.net/publication/266870946.

Hay GJ, Castilla G. 2006. Object-based image analysis: strengths, weaknesses, opportunities and threats (SWOT), Proceedings from 1st International Conference on Object-based Image Analysis, July 4–5, Salzburg, Austria.

Hofmann P. 2001. Detecting urban features from IKONOS data using an object oriented approach. *First Annual Conference of the Remote Sensing & Photogrammtery Society*, Sep 12–14, pp. 28–33.

Kim M, Madden M, Warner TA. 2009. Forest type mapping using object-specific texture measures from MS IKONOS imagery: segmentation quality and image classification issues. Photogramm Eng Remote Sensing. 75(7):819–829.

Li G, Lu D, Moran E, Hetrick S. 2011. Land-cover classification in a moist tropical region of Brazil with Landsat TM imagery. Int J Remote Sens. 32(23):8207–8230.

Liu D, Xia F. 2010. Assessing object-based classification: advantages and limitations. Remote Sens Lett. 1(4):187–194.

Makinde EO, Salami AT, Olaleye JB, Okewusi OC. 2016. Object based and pixel based classification using Rapideye satellite imagery of Eti-Osa, Lagos, Nigeria. Geoinformatics FCE CTU. 15(2):59–70.

Martin M, Lucie Z. 2014. Forest mapping through object-based image analysis of multispectral and LiDAR aerial data. Eur J Remote Sens. 47(1):117–131.

Mitchell M, Wilson RR, Twedt DJ, Mini AE, James JD. 2016. Object-based forest classification to facilitate landscape-scale conservation in Mississippi Alluvial Valley. Remote Sens Appl Soc Environ. 4(2016): 55–60.

Moran EF. 2010. Land Cover classification in a complex urban-rural landscape with QuickBird Imagery. Photogramm Eng Remote Sens. 76(10):1159–1168.

Piazza GA, Vibrans AC, Liesenberg V, and, Refosco JS. 2016. Object-oriented and pixel-based classification approaches to classify tropical successional stages using airborne high–spatial resolution images. GIScience & Remote Sensing. 53:206–226.

Sentinel-2 User Handbook 2015. ESA Standard Document, ESA, pp. 64.

Tsogtbaatar J. 2002. Forest Policy Development in Mongolia, IUFRO Science/Policy Interface Task Force regional meeting, Chennai, India at the M.S. Swaminathan Research Foundation.
Yan WY, Shaker A, Ashmawy NE. 2015. Urban land cover classification using airborne LiDAR data: a review. Remote Sens Environ. 158:295–310.
Weih, R.C. and Riggan, N.D., 2012. Object-based classification vs. pixel-based classification: comparative importance of multi-resolution imagery, The International Archives of the Photogrammetry, Remote Sensing and Spatial Information Sciences, Vol. XXXVIII-4/C7.
Wulder MA, Franklin SE, White JC, Linke J, Magnussen S. 2006. An accuracy assessment framework for large-area land cover classification products derived from medium-resolution satellite data. Int J Remote Sens. 27(4):663–683.
Zhang Y, Maxwell T, Tong H, Dey V. 2010. Development of a supervised software tool for automated determination of optimal segmentation parameters for eCognition, ISPRS TC VII Symposium – 100 years ISPRS, Vienna, Austria, July 5–7, 2010.